ANALYSIS OF THE ANISOTROPY FOR 3D PRINTED PLA PARTS USABLE IN MEDICINE

Sebastian GRADINARU[1], Diana TABARAS[2], Dan GHEORGHE[2]*, Daniela GHEORGHITA[2], Raluca ZAMFIR[2], Marius VASILESCU[2], Mircea DOBRESCU[2], Gabriel GRIGORESCU[2], Ioan CRISTESCU[3]

Given the production method used in additive manufacturing (successive layers build-up) anisotropy is to be expected. This study is oriented on the anisotropy of the mechanical properties in compression for 3D printed parts made of PLA that are used for medical applications. The ratio of elastic modulus on longitudinal to the transverse direction was found to be 0.48 and 0.59 for the yield strength, showing that an accentuated anisotropy appears.

Thermal processing was performed in order to ameliorate the anisotropy and the ratio value was risen to 0.73 for the elastic modulus and 0.86 for the yield strength.

Keywords: 3D printing, anisotropy, mechanical properties

1. Introduction

Additive manufacturing (AM) is used to describe a process where a part or even a whole system is rapidly created. The basic principle of this technology is that a model created using a Computer Aided Design (CAD) software can be fabricated directly by successive material addition. Initially the model was used solely for visualization purposes and current technology and material improvement allows the output to be suitable for end use.

Current AM technologies specified by ASTM F2792 are binder jetting, directed energy deposition, material extrusion, material jetting, powder bed fusion, sheet lamination and Vat polymerization, each with its own targeted fields.

In the medical field AM is an emerging technology [1] with wide use in personalized implant design and manufacture [2,3].

Of widespread in medical implant fabrication are extrusion-based systems that use the extrusion process to form parts.

[1] "Carol Davila" University of Medicine and Pharmacy Bucharest, Romania
[2] University POLITEHNICA of Bucharest, Romania, e-mail: dan.gheorghe@upb.ro
[3] Department of Orthopaedy & Traumatology, Clinical Emergency Hospital, Bucharest, Romania

The basic stages for the extrusion-based systems, as described in Fig.1, are: filament material loading using a feeding system, its liquefaction in a liquefier chamber then moved under pressure through a nozzle, extrusion and plotting in a controlled manner on a specified path. The extruded material bonds to itself or other materials and forms a coherent structure.

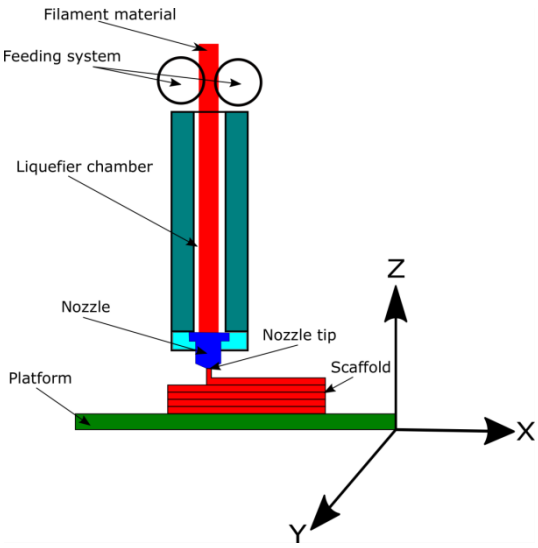

Fig. 1. The principle of 3D printing

The properties of filament materials need to comply to the manufacturing process as well as to finished product requirements. For medical applications the copolymers of polyglicolic acid (PGA) and polylactic acid (PLA) are most used given their history in use for sutures, scaffolds and biodegradable fixation materials [4-7], while new emerging composites (scaffolds of absorbable polymers with cell and osteo-inductive agents) usable as filament materials are developed [8-16].

PLA are biodegradable thermoplastic aliphatic polyesters, semi-crystalline in nature with melting temperatures of 200-205°C and a glass transition temperature of approximately 58°C. Their ultimate tensile strength is 25-50MPa with a low elastic modulus of circa 4GPa [17] when processed by injection molding.

Polymer processing methods and their parameters are known to alter their characteristics [18-20], thus a study regarding the printed and processed PLA is required, especially when its use is for structural applications.

2.Materials and methods

The generic additive manufacturing stages employed for sample fabrication are shown in Fig. 2. A CAD model is required then it is converted into a STL file which is manipulated and transferred to the machine where the part is built, removed, post-processed (usually de-burred) and prepared for application.

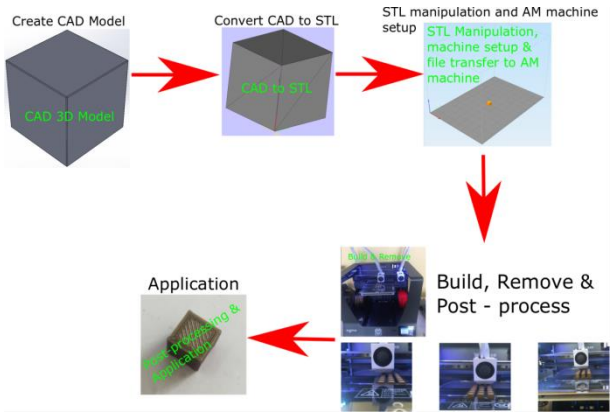

Fig. 2 Sample processing route

In this study the test samples were obtained by 3D printing using a CuraBCN3D Sigma 3D printer using as filament poly-lactic acid (PLA). Printing parameters were kept constant for all samples: the infill was set to 100% with a rectilinear pattern with ±45° infill angles, 5 top and bottom solid layers and 3 perimeter outlines, as depicted schematically in Fig. 3.

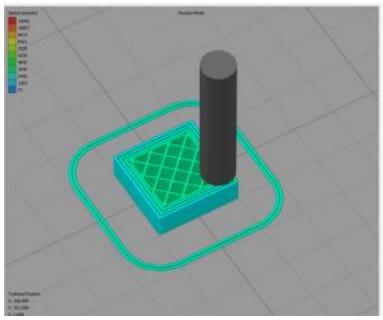

Fig. 3 Machine set-up parameters and tool-head travel during sample printing

In total 40 test samples shaped as cubes (10x10x10mm) were printed using the above-mentioned 3D printer parameters. The CAD model and a finished 3D printed sample are shown in Fig. 4along a detail during 3D printing.

a. b. c.

Fig. 4 Details showing the a. CAD model, b. samples during 3D printing and c. experimental sample

The obtained test samples were then separated into 4 batches, each comprising 10 specimens. One batch was used as reference, two were thermally processed by heating at 90°C in boiling water and in an electric furnace, held at this temperature for 60min and air cooled while the last was melted at the surface using a heat gun until individual layers were no longer visible. Sample coding along the processing parameters are mentioned in Table 1.

Table 1

Sample coding and processing

Sample coding	Processing
R	As printed, no processing
TP1	Water heating at 90°C/held 60min at 90°C/air cooling
TP2	Furnace heating at 90°C/held 60min at 90°C/air cooling
TP3	Superficial melting using a heat gun/air cooling

On the samples a dimensional analysis was performed by measuring the dimensions of a sample using a digital caliper with ±0.01mm resolution. One sample was randomly extracted from each batch and 18 length measurements were performed. The data was processed statistically and comparison against the reference sample was performed.

Using an Olympus BX51 light microscope the sample surface was studied. Using the microscope proprietary software layer thickness measurements were performed on randomly extracted samples and comparison was performed against the reference. The samples from TP3 batch was excluded from this investigation since the superficial melting process obscured individual layers.

Compression tests were performed using a hydraulic universal testing machine Walter+Bai LFV 300. The samples from each batch were devised in two subsets depending on the 3D printing direction (material build-up): parallel or perpendicular. The resulting force-displacement curves were processed in order to determine the mechanical characteristics (elastic modulus and yield strength in compression). An anisotropy coefficient was computed by dividing the property determined in one direction against the one determined on the perpendicular direction.

3. Results and discussion

3.1. Dimensional analysis of samples

On a random extracted sample from each batch 18 length measurements were performed using a digital caliper, this procedure being similar to a computerized dimensional analysis performed by Pantea [21] on connector diameters for fixed partial dentures. The results were recorded and processed, the box-plot presented in Fig. 5 shows the results.

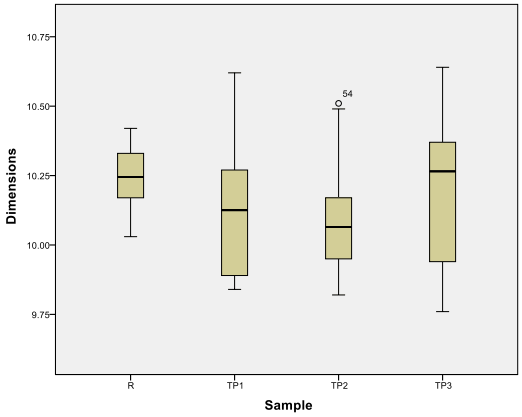

Fig. 5 Box-plot showing the spread of data for the dimensional analysis

From Fig. 5 it can be seen that reference sample R has the lowest while the surface melted sample TP3 has the greatest dataspread, still within acceptable tolerances for most applications.

A t-Test for two sample assuming unequal variances was performed with a null hypothesized mean difference using α=0.05. The test was performed in pairs by comparing R with TP1, R with TP2 and R with TP3.The results are shown in Table 2.

Table 2

The results of the t-Test

Pair	Hypothesized mean difference	t-Statistic	Significance
R-TP1	0	1.64	0.114
R-TP2	0	2.57	0.016
R-TP3	0	0.54	0.597

Statistical significant differences do not appear in the case of R-TP1 and R-TP3, thus dimensional variation does not appear when processing is performed in boiling water and superficial melting using a heat gun. Significant dimensional variations in sample dimensions, from statistical point of view, appear when heating is performed in an electric furnace.

3.2 Study of layer thickness

Using the Olympus BX51 light microscope images on the surfaces of a random extracted sample were obtained, a selection being presented in Fig. 6. The heat gun treated samples were not included in this test since individual layers could no longer be distinguished.

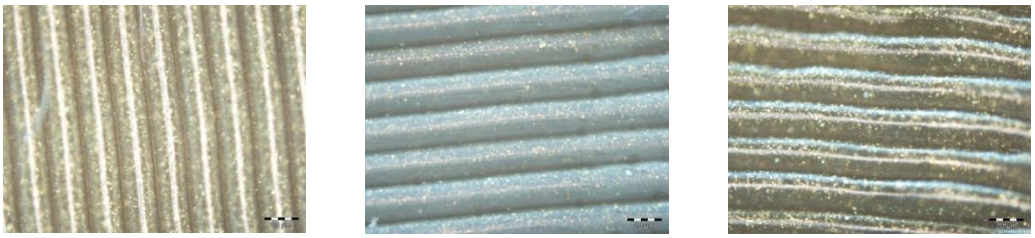

a. b. c.

Fig. 6 Light microscopy image showing layers in the 3D printed material for a. R, b. TP1 and c. TP3 samples

Individual layers can be observed, fused together generating a structure similar to a multi-ply composite. Also, a discoloration of sample TP1 can be noticed which could alter biologic performance [22].

Using the proprietary software of the light microscope 10 layer thickness measurements were performed on random regions of the micrograph. In Table 3 the descriptive statistics parameters are presented for the gathered data.

Table 3

Descriptive statistics parameters regarding the layer thickness

Sample	N	Mean [µm]	Standard deviation [µm]	Confidence interval of the mean [µm]
R	10	20.93	1.78	1.10
TP1	10	19.95	2.25	1.39
TP2	10	21.55	3.56	2.21

At first glance the results obtained showed a layer thickness reduction when heating was performed in water (sample TP1) and an increase when the furnace was used (sample TP2). Still, given the large standard deviation a t-Test for two samples assuming unequal variances was performed with a null hypothesized mean difference using α=0.05. The t-Test results are shown in Table 4.

Table 4

The results of the t-Test

Pair	Hypothesized mean difference	t-Statistic	Significance
R-TP1	0	0.763	0.457
R-TP2	0	-0.924	0.372

The results of the t-Test reveal that there are not statistically significant differences between the means, it cannot be assumed that layer thickness is influenced by thermal processing.

3.3 Compression tests

Compression tests were performed on a hydraulic universal testing machine Walter+Bai LFV 300 using a crosshead speed of 5mm/min.

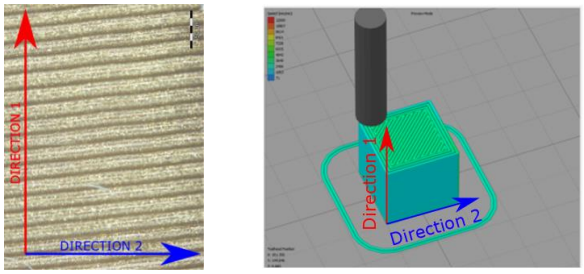

a. b.

Fig. 7 Sampling direction choice based upon a. material buildup and b. 3D printing process

In respect to material buildup during 3D printing process "Direction 1" was chosen to be the same as buildup direction and "Direction 2" was taken perpendicular as described in Fig. 7. The samples in each batch were divided in two to obtain 5 samples per direction to be tested in compression. Post testing the load-displacement curves were processed in order to determine the elastic modulus and yield strength in compression. The elastic modulus was determined by linear regression on the initial region of the stress-strain curve and the yield strength in compression was determined using the same procedure as the conventional yield strength in tension. In Fig. 8 the mediated stress - strain curves in compression for the 4 batches are presented.

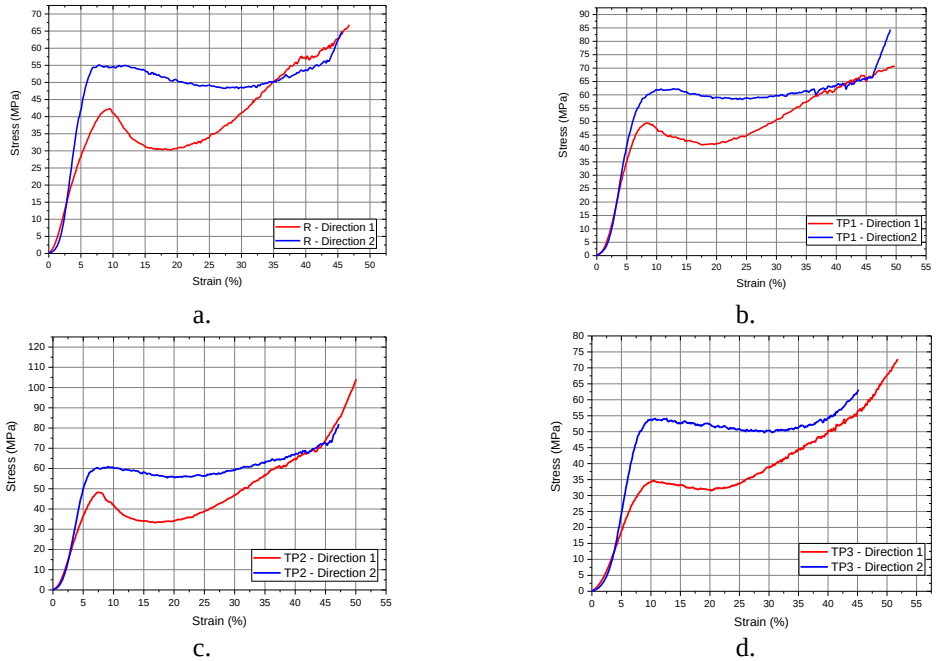

a. b.

c. d.

Fig. 8 Mean stress - strain curves in compression for samples from a. R, b. TP1, c.TP2 and d. TP3 batch

The curves suggest a malleable material with direction dependant behavior. It can be seen on the stress-strain curves in compression when the specimen is oriented on "Direction 1" that after reaching the first maxima a steeper decrease appears when compared with the specimen tested on "Direction 2."

Perpendicular layers on the load direction are compressed, slide against each other, the sample barrels and fails by separation of layers. When the load is parallel with the layers failure occurs by buckling of the perimeter layers (the outer ones) and the rectilinear infill oriented at ±45° significantly increase shear strength. Thermal processing appears to have an influence on the behavior, the difference between first maxima decreases when compared with the reference samples.

In case of specimens from TP3 batch it can be seen that the drop beyond the first maxima on "Direction 1" almost disappears, the outer layers are fused together and failure occurs in this case mainly by buckling.

In Fig. 9 comparisons between elastic moduli and yield strengths in compression are shown.

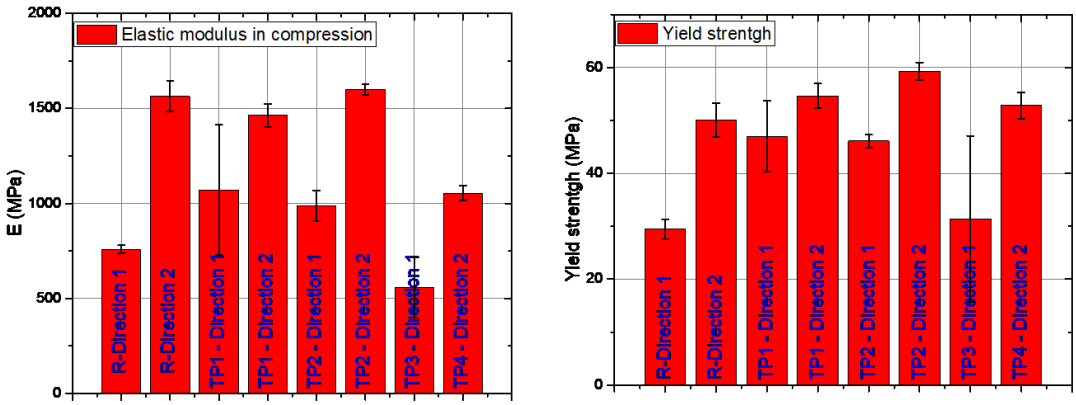

a. b.

Fig. 9 Comparison of a. elastic moduli and b. yield strength in compression

Analyzing the results from Fig. 9 it can be seen that the elastic modulus for the reference R samples in direction 2 is by 51.51% higher than the one on direction 1, for the samples TP1 the elastic modulus on direction 2 is by 26.84% higher than for direction 1, for samples TP2 the elastic modulus on direction 1 is by 38.24% higher than for direction 2 and for samples TP3 on direction 1 the elastic modulus is by 47.02% higher than the one in direction 2. For yield strengths the same pattern is observed, in direction 2 higher values are observed, for R samples direction 2 shows a value by 41.24% higher, for sample TP1 is by

13.98% higher, for samples TP2 by 22.30% higher and for samples TP3 by 40.58% higher.

It also can be stated that thermal processing clearly alters the structure of the 3D printed material, but the mechanisms were not studied. It was inferred that either adhesion between layers was improved or a change in the crystallinity degree of the polymer could be responsible. Using the furnace showed best results when the yield strength is in question and noteworthy is that the improvement on direction 1 is more pronounced than on direction 2, suggesting that processes at the interface of the layers is a stronger influence factor.

Using the heating gun for superficial melting of the samples did not yield good results; the process was performed using visual appreciation without specific process parameters. The process was halted when no more layers were observed on the surface thus process optimization is required for repeatability and reproducibility. The behavior during deformation associated with the mechanical characteristics values determined showed that 3D printed materials show anisotropy induced by the production characteristics, layer by layer build-up.

To appreciate the anisotropy and thermal processing influence on this aspect an anisotropy coefficient was determined by dividing the property value obtained on "Direction 1" to the one in "Direction 2", exemplified in eq. (1) for the yield strength:

$$Anistropy\ coefficient\ for\ yield\ strength = \frac{Yield\ strentgh\ on\ direction\ 1}{Yield\ strentgh\ on\ direction\ 2} \quad (1)$$

A comparison of the anisotropy coefficient for the elastic moduli and yield strengths in compression is shown in Fig. 10.

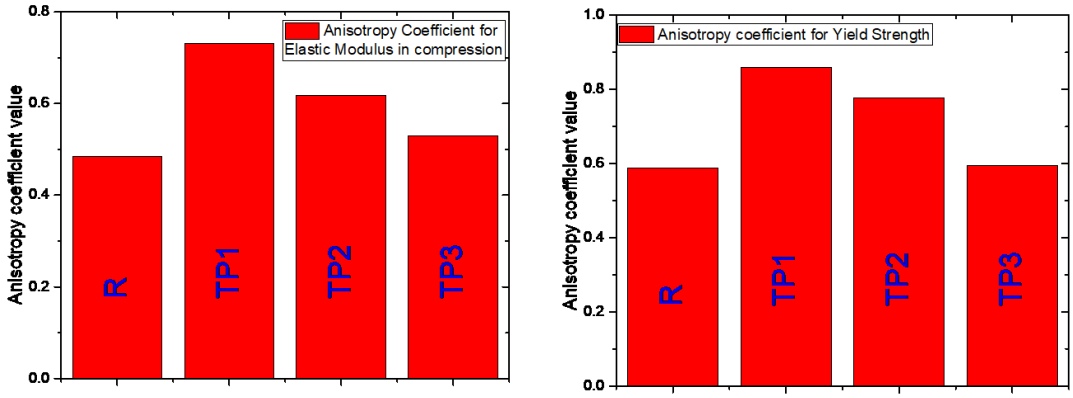

a. b.

Fig. 10 Anisotropy coefficient for a. elastic moduli and b. yield strengths in compression

For an isotropic material the value of this coefficient should be 1 in theory and very close to 1 using experimental data while in the case of 3D printed materials it is 0.49 for the elastic modulus and 0.59 for the yield strength in compression. Thermal processing improves the values for this coefficient getting it closer to 1 and highest values were obtained for sample TP1, processed in boiling water.

Several studies [23, 24, 25]reportslight variations of the elastic modulus in tension in XY plane (the transverse plane), with anisotropy coefficients ranging 0.92 to 0.98 as computed using the published values. Using this information associated with current results it can be assumed that 3D printed PLA is transversely isotropic, the strength and stiffness are greater when the samples are loaded perpendicular than when load is applied parallel in respect to the build-up direction.

3. Conclusions

This study was focused mainly on the mechanical characteristics of 3D printed materials targeted for medical applications. Samples made of PLA were printed using a commercial dual head extruder machine and processed by heating in boiling water, in a furnace and using a heating gun. Comparing sample dimensions, it was found that when using treatment in boiling water and using a heating gun no statistical significant differences between the their dimensions and the reference samples appear, while furnace heating generates dimensional variation. Using the same procedure layer thickness measurements were performed on optical micrographs and slight layer thickness decrease when using water for heating and thickness increase when using the electric furnace were observed, but no statistical significant differences were found.

The compression tests were performed on samples oriented perpendicular and parallel to the build-up directions of the 3D printed part. The compression test results confirmed that 3D printed materials are anisotropic and thermal post-processing can reduce anisotropy. In this study it was observed that when heating in performed in water the anisotropy is reduced, but not the best mechanical characteristics are achieved - furnace heating gave best mechanical characteristics.

Material anisotropy should not be regarded as an inconvenient (it depends upon the final application and sometimes anisotropy is desired). Careful planning before 3D printing should be performed to align the part with the direction that gives best mechanical characteristics for the application.

REFERENCES

[1] *Salmi, M.; Paloheimo, K. S.; Tuomi, J.; Wolff, J.; Makitie, A.*: Accuracy of medical models made by additive manufacturing (rapid manufacturing). J CranioMaxillSurg2013, **41**, 603-609

[2] *Paun, M. A.; Frunza, A.; Stanciulescu, E. L.; Munteanu, T. C.; Cristescu, I.; Grama, S.; Chiotoroiu, A.; Ene, A.; Mihai, C.*: The use of collagen-coated polypropylene meshes for nasal reconstructive surgery. IndTextila2019, **70**, 242-247

[3] *Antoniac IV, Stoia DI, Ghiban B, Tecu C, Miculescu F, Vigaru C, Saceleanu V.:* Failure Analysis of a Humeral Shaft Locking Compression Plate—Surface Investigation and Simulation by Finite Element Method. Materials. 2019; **12(7)**:1128

[4] *Lasprilla, A. J. R., Martinez, G. A. R., Lunelli, B. H., Jardini, A. L., &Filho, R. M*. (2012). Poly-lactic acid synthesis for application in biomedical devices - A review. Biotechnology Advances. https://doi.org/10.1016/j.biotechadv.2011.06.019

[5] *Raquez, J. M., Habibi, Y., Murariu, M., & Dubois, P. (2013)*. Polylactide (PLA)-based nanocomposites. Progress in Polymer Science. https://doi.org/10.1016/j.progpolymsci.2013.05.014

[6] *Elsawy, M. A., Kim, K. H., Park, J. W., & Deep, A*. (2017). Hydrolytic degradation of polylactic acid (PLA) and its composites.Renewable and Sustainable Energy Reviews. https://doi.org/10.1016/j.rser.2017.05.143

[7] *Vilcioiu, J. D.; Zamfirescu, D. G.; Cristescu, I.; Ursache, A.; Popescu, S. A.; Creanga, C. A.; Lascar, I.*: The interdisciplinary approach of an aggressive giant cell tumor of bone complicated with a fracture of the distal femur. Rom J Morphol Embryo2016, **57**, 567-572

[8] *Petreus, T.; Stoica, B. A.; Petreus, O.; Goriuc, A.; Cotrutz, C. E.; Antoniac, I. V.; Barbu-Tudoran, L.*: Preparation and cytocompatibility evaluation for hydrosoluble phosphorous acid-derivatized cellulose as tissue engineering scaffold material. J Mater Sci-Mater M2014, **25**, 1115-1127

[9] *Guazzo, R.; Gardin, C.; Bellin, G.; Sbricoli, L.; Ferroni, L.; Ludovichetti, F. S.; Piattelli, A.; Antoniac, I.; Bressan, E.; Zavan, B.*: Graphene-Based Nanomaterials for Tissue Engineering in the Dental Field. Nanomaterials-Basel2018, **8**

[10] *Rau, J. V.; Antoniac, I.; Cama, G.; Komlev, V. S.; Ravaglioli, A.*: Bioactive Materials for Bone Tissue Engineering. Biomed Res Int2016

[11] *Tecu, C.; Antoniac, I.; Goller, G.; Yavas, B.; Gheorghe, D.; Antoniac, A.; Ciuca, I.; Semenescu, A.; Raiciu, A. D.; Cristescu, I.*: The Sintering Behaviour and Mechanical Properties of Hydroxyapatite - Based Composites for Bone Tissue Regeneration. Mater Plast2019, **56**, 644-648

[12] *Antoniac, I.; Popescu, D.; Zapciu, A.; Antoniac, A.; Miculescu, F.; Moldovan, H.*: Magnesium Filled Polylactic Acid (PLA) Material for Filament Based 3D Printing. Materials2019, **12**

[13] *Niculescu, M.; Antoniac, A.; Vasile, E.; Semenescu, A.; Trante, O.; Sohaciu, M.; Musetescu, A.*: Evaluation of Biodegradability of Surgical Synthetic Absorbable Suture Materials: An In Vitro Study. Mater Plast2016, **53**, 642-645

[14] *Titorencu, I.; Albu, M. G.; Giurginca, M.; Jinga, V.; Antoniac, I.; Trandafir, V.; Cotrut, C.; Miculescu, F.; Simionescu, M.*: In Vitro Biocompatibility of Human Endothelial Cells with Collagen-Doxycycline Matrices. MolCrystLiqCryst2010, **523**, 82-96

[15] *Ionescu, M. A.; Ionescu, C.; Ciocoiu, R. C.; Ciuca, I.*: Parylene-N a Better Candidate for Medical Substrate Coating than Parylene-C. Rev Chim-Bucharest2015, **66**, 1925-1928

[16] *Dascalu, C. A.; Maidaniuc, A.; Pandele, A. M.; Voicu, S. I.; Machedon-Pisu, T.; Stan, G. E.; Cimpean, A.; Mitran, V.; Antoniac, I. V.; Miculescu, F.*: Synthesis and characterization of

biocompatible polymer-ceramic film structures as favorable interface in guided bone regeneration. Appl Surf Sci2019, **494**, 335-352

[17] *Senatov, F. S., Niaza, K. V., Zadorozhnyy, M. Y., Maksimkin, A. V., Kaloshkin, S. D., & Estrin, Y. Z.* (2016). Mechanical properties and shape memory effect of 3D-printed PLA-based porous scaffolds. Journal of the Mechanical Behavior of Biomedical Materials. https://doi.org/10.1016/j.jmbbm.2015.11.036

[18] *Moldovan, M.; Balazsi, R.; Soanca, A.; Roman, A.; Sarosi, C.; Prodan, D.; Vlassa, M.; Cojocaru, I.; Saceleanu, V.; Cristescu, I.*: Evaluation of the Degree of Conversion, Residual Monomers and Mechanical Properties of Some Light-Cured Dental Resin Composites. Materials2019, **12**,

[19] *Rivis, M.; Pricop, M.; Talpos, S.; Ciocoiu, R.; Antoniac, I.; Gheorghita, D.; Trante, O.; Moldovan, H.; Grigorescu, G.; Seceleanu, V.; Mohan, A.*: Influence of the Bone Cements Processing on the Mechanical Properties in Cranioplasty. Rev Chim-Bucharest2018, **69**, 990-993

[20] *Bolcu, D.; Stanescu, M. M.; Ciuca, I.; Trante, O.; Mihai, B.*: New Relations for the Calculus of Elastical and Mechanical Characteristics of Polyester Composites Reinforced with Randomly Dispersed Fibers. Mater Plast2009, **46**, 206-210

[21] *Pantea, M.; Antoniac, I.; Trante, O.; Ciocoiu, R.; Fischer, C. A.; Traistaru, T.*: Correlations between connector geometry and strength of zirconia-based fixed partial dentures. Mater Chem Phys2019, **222**, 96-109

[22] *Antoniac, I.; Sinescu, C.; Antoniac, A.*: Adhesion aspects in biomaterials and medical devices. J AdhesSciTechnol2016, **30**, 1711-1715

[23] *T. Letcher, M. Waystanek*, Material property testing of 3D-printed specimen in PLA on an entry-level 3D printer, ASME 2014 International Mechanical Engineering Congress&Exposition, ISBN 978-0-7918-4643-8, 2015

[24] *Tymrak, B. M.; Kreiger, M.; Pearce, J. M.*: Mechanical properties of components fabricated with open-source 3-D printers under realistic environmental conditions. Mater Design2014, **58**, 242-246

[25] *Serra, T.; Planell, J. A.; Navarro, M.*: High-resolution PLA-based composite scaffolds via 3-D printing technology. ActaBiomater2013, **9**, 5521-5530